AN EXPERIMENTAL STUDY ON FLOW AROUND TWO-DIMENSIONAL MODELS WITH REFERENCE TO BED FROM PORPAGATION

TAKEO NAKAGAWA and FUSETSU TAKAGI

Department of Civil Engineering

(Received October 30, 1981)

Abstract

An experimental study on the flow around wavy models has been made. All of the models has two crests and two-dimensional profile. It is found that the flow instability around the models depends on the Reynolds number $R_\infty = U_\infty h / \nu$, where U_∞ is the free stream velocity, h the model height and ν the kinematic viscosity of the fluids, and the steepness $S = h / \lambda$, where λ is the model wave length, but the flow separation depends on the steepness only. Also, found are that on the surface of the models there appear Taylor-Görtler type vortices once the Reynolds number exceeds the critical value and that the form of the vortices is deformed depending on the Reynolds number and the model profile. On the basis of the present experiment, it is suggested that the intensity and scale of the separation eddy are decisive factors for bed form propagation.

CONTENTS

1. Introduction

Humankind has been fascinated by the peculiar formation of sand waves for many centuries. Extreamly complex interactions of sediment on the bed and motion of fluids have been unsurmountable barrier for viewing the complete picture of this subject.

It has been realized that in nature sediment is transported both upstream and downstream. Relating to this fact, Darwin[1] and Ayrton[2] have already noted importance of the flow separation for the bed form propagation. The more substantial evidences have been however, documented recently: The role of the flow separation on the bed form propagation has been discussed by Raudikivi[3, 4]. Karcz[5], a series work at University College, London[7, 8, 9] and others. All of them has discussed the interactions of the bed form and flow in the analogy of those of a single step and flow. It may be considered that such a model study is too crude.

Thus, in the present paper, for the more realistic study, two-dimensional models consisting of two crests placed one behind the other have been used and the detailed investigation about the flow around models has been made with close reference to the bed form propagation. The results will be given and discussed in this paper.

2. Apparatus

A towing system of the tank is used, so that the tow velocity on the model will be considered as the free stream velocity in the present experimental analysis, to be described. Schematic diagrams of the flow visualization experiments and pressure experiments are shown in Figs. 1 and 2, respectively. In the present
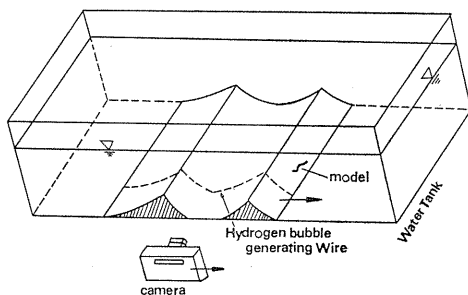

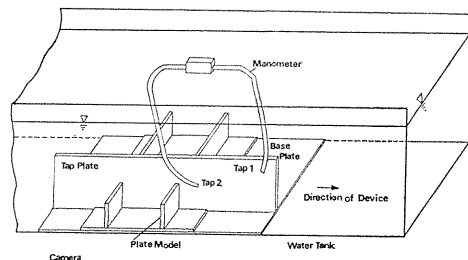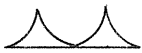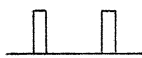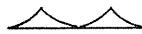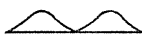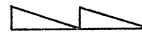Fig. 1. Schematic diagram of flow visualization experiments.

Fig. 2. Schematic diagram of pressure measurements.

experiments, two kinds of tanks have been used: The large tank is 14.64m length, 61.6 cm wide and 29.5cm deep, while the small tank is 9.17 m length, 23.0 cm wide and 35.0 cm deep. The two towing systems are, however, basically the same except their dimensions.

Table 1. Name, profile and dimensions of models.

Name of models	Profile	Wave length λ(cm)	Wave height h(cm)	Steepness h/λ
large mountain		10.0	5.0	0.5
medium mountain		6.25	3.125	0.5
small mountain		4.35	2.175	0.5
large plate		10.0	5.0	0.5
small plate		10.0	4.25	0.425
large crest		10.0	3.0	0.3
medium crest		10.0	2.5	0.25
small crest		10.0	1.0	0.1
Witch of Agnesi		8.0	2.8	0.35
large saw-tooth		10.0	3.0	0.3
small saw-tooth		10.0	1.0	0.1

In Table 1, listed are the name, profile and dimensions of all the models which are made of plexiglass. The experiments with the mountain and plate models have been done in the large tank, while the experiments with the crest, Witch of Agnesi and saw-tooht models have been done in the small tank.

Each of the tanks has parallel rails along which a carriage travels and the side walls are made of transparent glass, so that it is possible to observe motions of fluids around the models through the walls. The whole apparatus are driven by a motor through wire ropes. Speed of the carriage is controlled by a volt slider and is determined by measuring the time interval for the model to move a reference distance of 100.0 cm.

3. Method

3. 1. Flow visualization experiments

For the flow visualization, hydrogen bubbles and a patch of milk are used as the flow tracers. In performing the hydrogen bubble flow visualization experiment, the large tank is filled with water. The cathode is the hydrogen bubble generating copper wire of 0.082 mm attached on the surface of the model. The existence of the wire, therefore, may not disturb the flow around the model. The position of the wire is 15.5 cm from the observation wall and the direction of the wire is aligned to the two direction. On the other hand, the anode is the tin base plate, on which the model sits. When a DC potential is applied between the cathode and anode, tiny hydrogen bubbles appear on the surface of the wire due to the electrolytic action. These bubbles are used for the flow visualization.

On the other hand, in performing the milk flow visualization experiment, all the models are painted in black colour to sharpen the photographic contrast bet-

ween the milk and models. Then small amount of milk is put on troughs of the model before the model starts moving. It is soon realized that milk is a useful tracer to visualize motions of the fluid on the surface of the model, because the specific weight is only slightly greater than that of the water.

After the flow around the model is fully developed, photographs are taken by an observer moving with the model and by synchronizing the camera shutter with an electronic flash which illuminates regions of interest through a thin slit, keeping the background as dark as possible.

Once the flow in the separation eddy becomes unstable, clear hydrogen bubble lines change into chaotic pieces, while the milk delineates the three-dimensional texture of the flow on the surface of the model. These characters of the present tracers have been used for determining critical conditions of the flow instability in the separation eddy.

3. 2. Pressure measurements

Streamwise pressure distributions around the large mountain model and large plate model have been measured to know how the distributions depend on the model profile and the Reynolds number.

The pressure manometer combines an optical velocity measurement with the Hagen-Poiseulle relation to infer the pressure difference. The pressure difference between both ends 1 and 2 of a pipe is

$$p_1 - p_2 = 4\mu L u_m / R^2,$$

where μ is the dynamic viscosity of the fluid, L the pipe length, u_m the maximum velocity in the pipe and R the pipe radius. Since μ, L and R are given, a measurement of u_m provides a constant pressure difference between two points in the fluid. For a more detailed description of the pressure manometer, refer to the original papers.[10, 11]

The pressure tap plate is mounted as shown in Fig. 2 for the large plate model. For the large mountain model, another pressure tap plate fitted to the model profile is used. The pressure at tap 1 is chosen as the reference and each value of the pressures, to be plotted, is obtained by averaging the 13 data.

4. Results

4. 1. General features of flow around models.

Figure 3 shows criteria of the flow instability in the separation eddy is laminar and turbulent, respectively. It is clear that the flow instability depends on both the Reynolds number and the steepness of the model, and that the flow around the models does not separate if the steepness is smaller than 0.1, but the flow will separate if the steepness is larger than 0.1. Note that even though the steepness is smaller than 0.1, it is certain that a small separation eddy will be generated behind each discontinuity (or roughness) of the model profile. However, if these small separation eddies are not of significance for the flow around the model, it is classified in the present paper that the flow does not separate. It is also clear in Fig. 3 that the separation eddy becomes turbulent at the lower Rey-
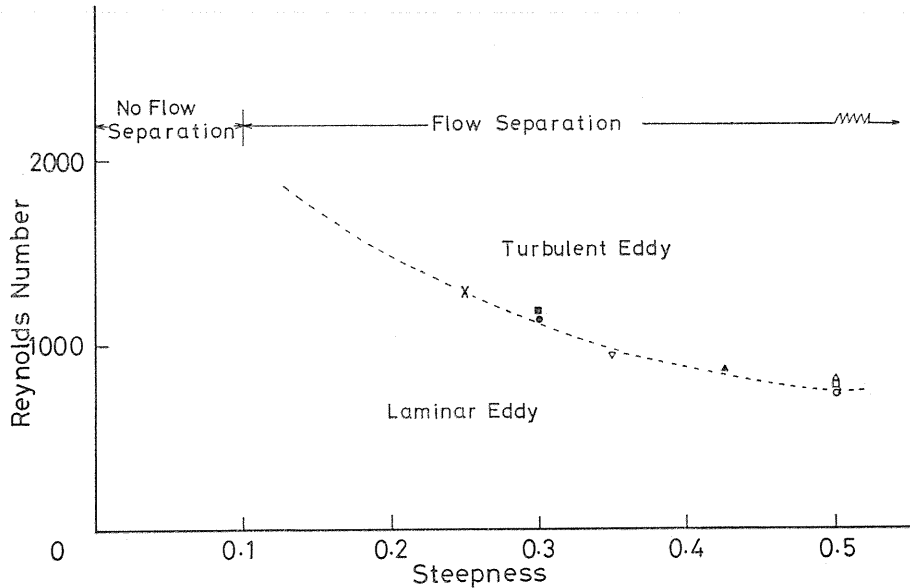
Fig. 3. Criteria of flow instability in separation eddy and flow separation
       around models.
       ○ : large mountain,   △ : medium mountain,   □ : small mountain,
       ▓ : large crest,   × : medium crest,   ▽ : Witchof Agnesi,
       ▲ : small plate,   ◉ : large saw-tooth

nolds number as the steepness is increased.

In the case of the mountain models and plate models, the flow always sepa-
rates from the front crest and reattaches at the following rear crest.   The re-
attached flow, then recirculates in the separation eddy.   On the other hand, in the
case of large and medium crest models, Witch of Agnesi model and large sawtooth
model, the flow separates from the front crest and then reattaches at a position
between the crests.   It is, therefore, that the degree of the flow separation and
scale of the separation eddy will be different from each other depending on the
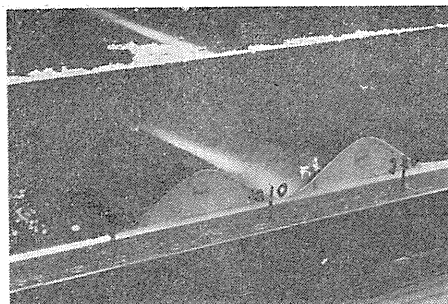steepness of the model and the Reynolds number.

Fig. 4. Parallel streak lines on the surface of the Withc of Agnesi model.
       The Reynolds number is below the critical value.
       The two direction is from left to right.

When the Reynolds number is smaller than the critical value, a patch of milk put on the through shows parallel streaklines as shown in Fig. 4. However, once the Reynolds number exceeds the critical value, three dimensional vortices appear

Fjg. 5(a). Taylor-Görtler type vortices on the surface of the large mountain model. $R_\infty = 978$.
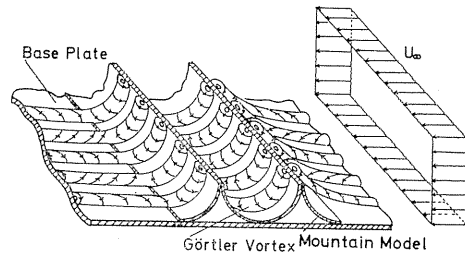The tow direction is from left to right.

Fig. 5(b). A sketch of Taylor-Görtler type vortices on the surface of mountain models.
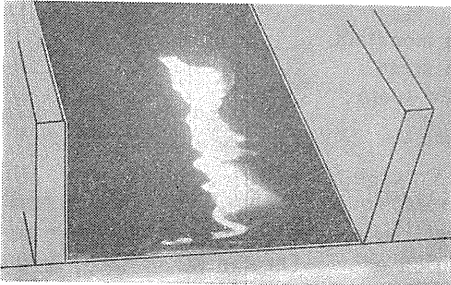

Fig. 6(a). Rayne-Lumley type cylindrical vertical vortices traced with milk on the trough of the large plate model. $R_\infty = 978$. The tow direction is from left right.
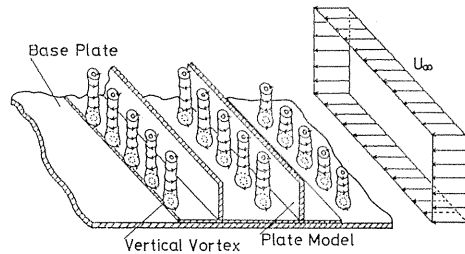

Fig. 6(b). A sketch of Payne and Lumley type cylindrical vertical vortices on the large plate models.

Fig. 7. Deformed Taylor-Görtler type vortices on the surface of the large crest model.
$R_\infty = 1123$. The tow direction is from left to right.
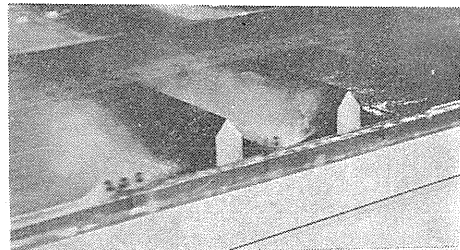

Fig. 8. Turbulent mixing of the milk around the large crest model.
$R_\infty = 2042$. The tow direction is from left to right.

during the transitional range of the Reynolds number. In the case of the mountain models, Taylor-Görtler type vortice have been observed over the concave semicircular wall as shown in Fig. 5, whereas in the case of the plate models, Payne-Lumley[13] type cylindrical vertical have been observed as shown in Fig. 6. Less defined Taylor-Görtler type vortices have been observed on the surface of the large and medium crest models, Witch of Agnesi model and large saw-tooth model. For example, Fig. 7 shows deformed Taylor-Görtler type vortices on the surface of the large crest model. If the Reynolds number exceeds the upper limit of the transitional range, the flow around the model becomes turbulent: Fig. 8 shows such a turbulent flow around the large crest model. It should be noted, however, that the both lower and upper limits of the transitional range are not sharply defined: for example, Fig. 9 provides the initiation of the cylindrical vortices traced with milk on the trough of the large plate model when the Reynolds number is slightly smaller than the critical value determined in the present experiment.
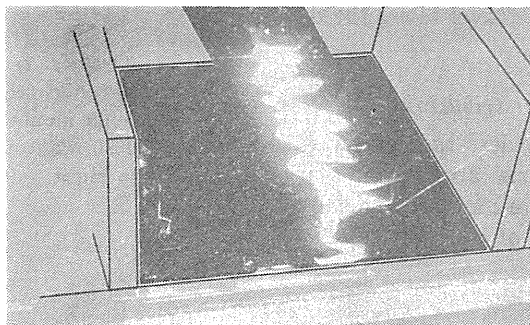
Fig. 9. Initiation of Payne-Lumley type vortices on the trough of
the large plate model.
$R_{\infty}=690$. The tow direction from left to right.

Fig. 10. A patch of the milk wiped-out by
the flow from the surface of the small
crest model.
$R_{\infty}=608$. Tow direction is from left
to right. Grey cloudy parts on the
photogrph show the milk swept down-
stream.

Fig. 11. Scouring of the stagnant milk
trapped in front of the vertical step
of the small saw-tooth model.
$R_{\infty}=593$. The tow direction is from
right to left.

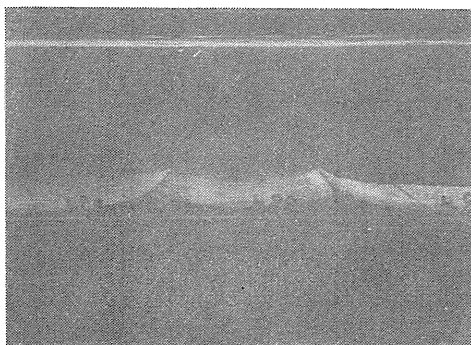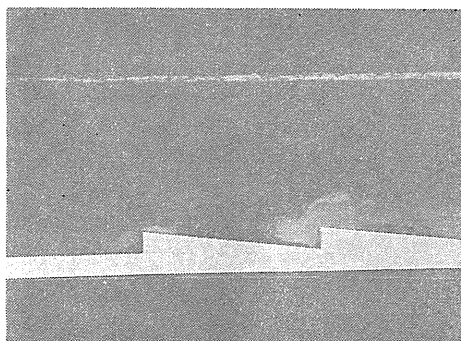On the other hand, when the steepness of the wavy model is smaller than the critical value, viz., 0.1, the flow around the models is carried downstream except the fluids in small flow separation regions behind the discontinuities of the model profile, irrespective of the value of the Reynolds number. Figures 10 and 11 provide such photographs. The former photograph and the latter photograph show that the milk put on the surface of the model is wiped out and scoured up by the flow in the downstream direction, respectively.

The motion of the fluids in the separation eddy is maintained by the shear stresses at the dividing free streamline mainly. Owing to the instability at the dividing free streamline, vortices with a horizontal axis have been generated. Figure 12 shows these vortices delineated by the hydrogen bubbles and the vortices are shed from the front crest of the large mountain model and travel along the dividing free stleamline.

Fig. 12. Vortices traced with hydrogen bubbles shed from the front crest of the large mouotain model.
$R_\infty = 1990$. The tow direction is from left to right.

4. 2. Pressure distributions

Figure 13 provides the streamwise pressure distributions around the large plate model and large mountain model and at the lower part of the figure shown
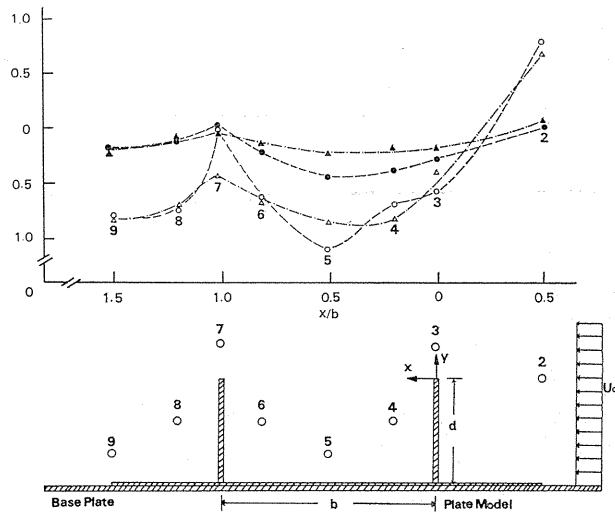

Fig. 13. Streamwise pressure distributions around the models.
Laminar eddy ($R_\infty = 526$)   : △ : large plate model,
                                          ○ : large mountain model,
Turbulent eddy ($R_\infty = 1692$) : ▲ : large plate model,
                                          ◉ : large mountain model.
The number besides the data denotes respective tap position.

are positions of the pressure taps 2–9. In Fig. 13, the open and filled triangular symbols denote the data for the laminar and turbulent eddy around the large plate model, respectively: While the open and filled circular symbols denote the data for the laminar eddy and turbulent eddy around the large mountain model, respectively. The abscissa of this figure is the distance normalized by the length of 100 mm between the crests and the ordinate is the normalized pressure difference in the form,

$$C_p = 2(p_1 - p_\infty)/(\rho U_\infty^2),$$

where p_∞ is the reference pressure at tap 1, p_i $(i=2–9)$ the pressure at a position at the tap plate, U_∞ the tow velocity of the model or the model or the free stream velocity and ρ the density of the water. It must be noted that irrespective of the laminar eddy or turbulent eddy the streamwise pressure distribution for the large mountain model has a more sharper negative peak than that of the large plate model at $x/b \doteqdot 0.5$, and the pressure distribution for the turbulent eddy is flatter than that for the laminar eddy due to the stronger turbulent mixing in the turbulent eddy.

5. Discussion

Bucher[14] has described that current-ripples travel downstream and the grains on the bed are rolled up the gentle weather-side slope and are dropped into the steep lee-side. Bucher[14] summarized the experimental data associated with current-ripples and showed that the steepness of the current-ripples ranged from 0.05 to 0.25 and that the typical Reynolds number R_∞ was 2.75×10^3.

The present study suggests that when the steepness of the current-ripples if smaller than 0.1, the sediment on the bed is carried by "scouring", which means that the sediment is lifted up by suction from the bed or "saltation" along the surface of current-ripples in the downstream direction only. The processes of the sediment transport around curren-ripples have been modeled by the present milk flow visualization experiment qualitatively. Figures 10 and 11 show such examples.

It is known that progressive sand waves or dunes travel downstream after the manner of wind-dunes or current-ripples. Bucher[14] collected the data concerning progressive sand-waves was 1.66×10^6. However, under the continual current progressive sand-waves are transported in such a way that the lee-side has an inclination of about 45 degrees, in strong contrast to the gentle weather-side (Partiot[15]). The form of progressive sand waves is also not stable at higher velocities. Partiot[15] observed that the sediment was carried beyond the slope on the lee-side: the height of the crest was rapidly reduced and the advance was greatly retarded. If the current velocity was not diminished in due time, the progressive sand wave often disappeared entirely.

It is important to note here that both the current-ripple and the progressive sand wave have a gentle weather-side and steep lee-side, in which the steepness is normally smaller than 0.1. In these cases, the sediment is carried by scouring or saltation in the downstream direction and the sediment on these bed are eroded at the weather-side primarily.

It is suggested, here, the basic difference between the current-ripple and pro-

gressive sand wave is in its potential of scouring the sediment from the bed. The
typical Reynolds number of the flow around current-ripples is in order of 10^3,
while that of the flow around progressive sand waves is in order of 10^6. Thus
the eroded sediment from the weatherside of progressive sand waves may be kept
from falling by the scouring, while that from the weather-side of currentripples
may follow the bed surface. Suggested flow patterns over the various wavy profiles
that have the steepness smaller than 0. 1, have been depicted in Fig. 14.
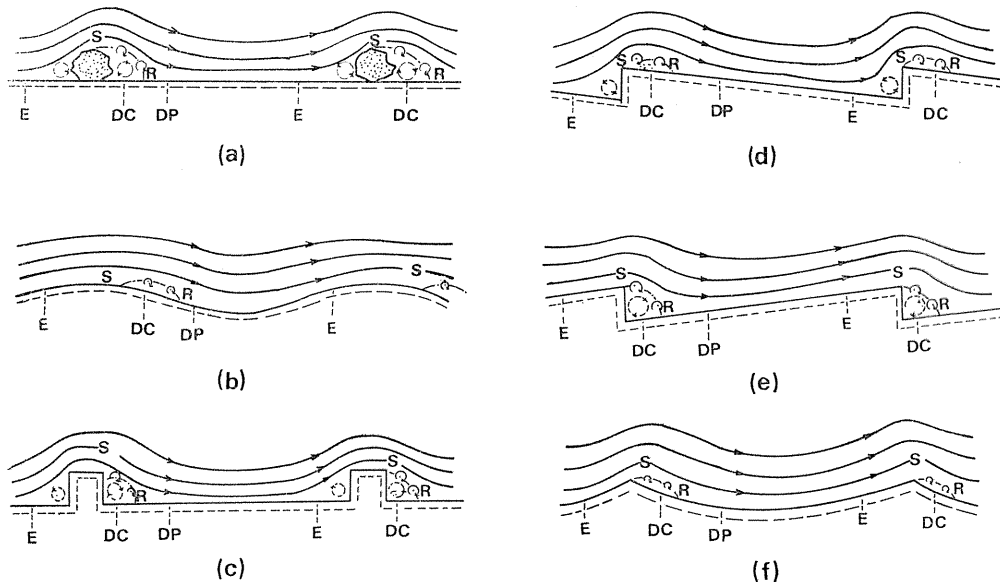

Fig. 14. Suggested flow patterns over the wavy beds when the steepness is smaller
than the critical value.
(a)   wavy bed profile formed by rocks,
(b)   bed profile of current-ripples or progressive sand waves,
(c)   tooth bed profile,
(d)   saw-tooth bed profile, where the vertical wall faces the free stream,
(e)   saw-tooth bed profile, where the inclined wall faces the free stream,
(f)   sharp crested bed profile.
S : separation point, R : reattachement point, E : eroded area, DC :
deposited area of current-ripples, DP : deposited area of progressive
sand-waves.
The small vortices along the dividing free streamline show vortices shed
from the crest.

Regressive sand waves (or anti-dunes) owe their name due to the fact that
their forms travel upstream. Gilbert[16] has observed that at the crest, sand grains
have up and down motions, especially on the crest of the larger regressive sand
waves their forward motions are small compared with their vertical motions.
Gilbert's[16] observations may suggest the existence of a strong separation eddy
behind the crest.
    It has been reported by Bucher[14] that the steepness of regressive sand waves
ranges from 0. 30 to 0. 40 and the Reynolds number of the flow around regressive

sand waves is in order of 10^6. The present study suggests that when the steepness of wavy models is larger than 0.1, a separation eddy occupies the significant part of the space between the crests. The flow around regressive sand waves may separate and reattach at a position on the weather-side of the following sand wave, though the actual position depends on the flow conditions and the form of the sand wave. Suggested flow pattern around the various regressive sand waves have been depicted in Fig. 15. Both of the areas in front and rear of the reattachment
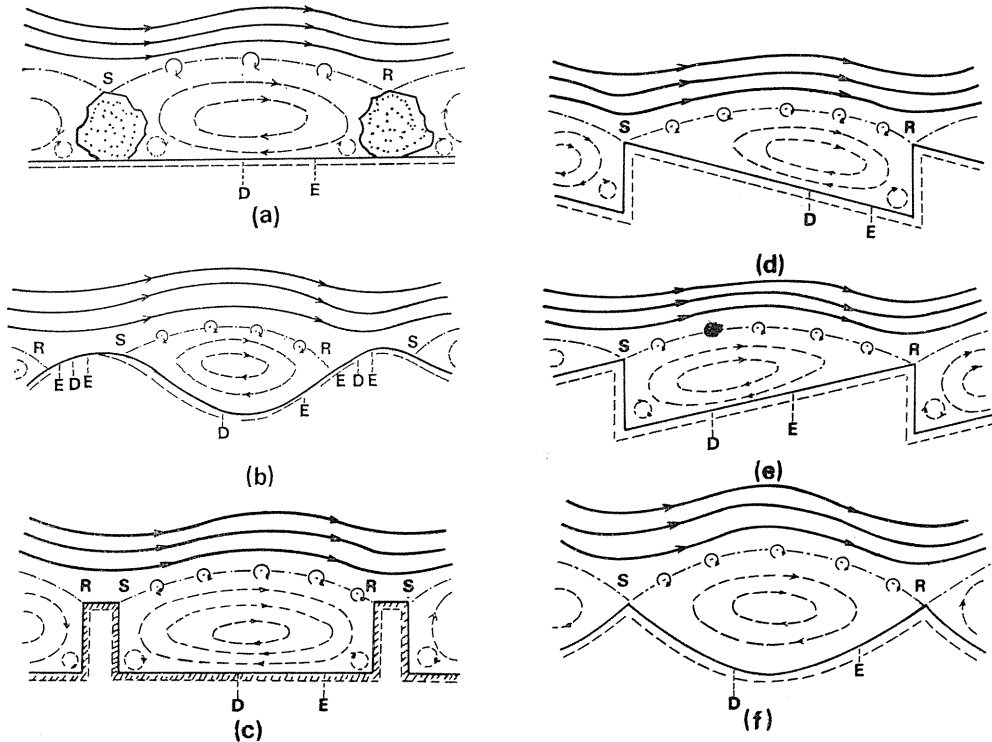
Fig. 15. Suggested flow patterns over the wavy beds when the steepness is larger than the critical value. See Fig. 14. for legend and replace parts of the legend in Fig 14. as follows. (b) bed profile of regressive sand waves, D: deposited area.

point will bd eroded by the higher velocity along the dividing free streamline (Riabouchinsky[17]). The eroded sediment from the area in front of the reattachment point will be deposited at a area just behind the separation point mainly, but some part of the eroded sediment may go out from the separation eddy by the momentum transfer across the dividing free streamline. While, the eroded sediment at the area behind the reattachment point will be brushed away downstream by the flow, and then will be deposited on the surface of the weather-side of the following sand wave. Behind deposited area, there may be another area, to be eroded, by the free stream. Most of the sediment eroded from area will be transported over the following separation eddy and will be deposited on a area behind the following reattachment point. It is, therefore, expected that regressive sand

waves may tend to be flattened by the sediment transportation proesses described in the above. Indeed, it is known that regressive sand waves remain for several minutes only, and leave the surface of the bed without sand waves in nature (e. g. Bucher[14]).

6. Conclusions

It is found that flow instability around the two-dimensional wavy models depends on the Reynolds number and the steepness of the model, but flow separation depends on the steepness of the model only. It is also found that on the surface of the models Taylor-Görtler type vortices appear once the Reynolds number exceeds the critical value and the form of the vortices is deformed depending on the Reynolds number and model profile. Especially, in the case of the mountain model, having a concave semi-cirular wall between the crests, the well defined Taylor-Görtler vortices have been observed on the wall, whereas in the case of the plate model consisting of two vertical plates placed one behind the other, Payne and Lumley type vortices have been observed on the trough.

Finally, it is suggested that the intensity and scale of the separation eddy are decisive factors for the bed form propagation.

References

1) Darwin, G. H.: On the formation of ripple-mark in sand. Proc. Roy. Soc. London. A, 36, 18-43, 1883.

2) Ayrton, H.: On the origin and growth of ripple mark. Proc. Roy. Soc. London. A, 84, 285-310, 1910.

3) Raudkivi, A. J.: Study of sediment ripple formation, Proc. ASCE, HY6, paper 3692, 1963.

4) Raudkivi, A. J.: Bed forms in alluvial channels, J. Fluid Mech. 26, 507-514, 1966.

5) Karcz, I.: Reflections on the origin of some small-scale longitudinal stream bed scours. Fluvial Geomorphology (ed. by M. Morisawa), University of New York, Binghamton, 149-173, 1973.

6) Williams, P. B. and Kemp, P. H.: Initiation of ripples on flat sediment beds. Proc. ASCE, HY4, 97, paper 8042, 1971.

7) Williams, P. B. and Kemp, P. H.: Initiation of ripples by artificial disturbances. Proc. ASCE, HY6, 98, paper 8952, 1972.

8) Etheridge, D. W. and Kemp, P. H.: Measurements of turbulent flow downstream of a rearward-facing step. J. Fluid Mech. 86, 545-566, 1978.

9) Etheridge, D. W. and Kemp, P. H.: Velocity measurements downstream of rearward-facing steps, with reference to bed instability. J. Hyd. Res. 17. 107-119, 1979.

10) Nakagawa, T.: On flow and flow instability over concave walls with reference to sedimentation, Ph. D thesis, Department of Mechanical Engineering, Monash University, Victoria, Australia, 1979.

11) Nakagawa, T.: A device for measuring a low pressure difference. Trans. ASME, J. Fluid Eng. 102, 499-501, 1980.

12) Nakagawa, T.: Columnar vortices in cavity flow. Naturwissenschaften, 66, 468-469, 1979.

13) Payne, F. R. and Lumley, J. L.: Large eddy structure of the turbulent wake behind

a circular cylinder, Phs. Fluids, 10, s 194–196, 1967.

14) Bucher, W. H.: Oripples and related sedimentary surface forms and their paleo-geographic interpretation, Am. Jour. Sci. Fourth series, 47, 149–210, 1919.

15) Partiot, M.: Mémorie sur les sables de la loire, Ann des Ponts et Chaussesées 5, 1, 233–292, 1871.

16) Gilbert, G. K.: The transportation of debris by running water, U. S. Geol. Survey Prof. paper 86, 1914.

17) Riabouchinsky, D.: On steady fluid motions with free surfaces, Proc. London Math. Soc. (2), 19, 206–215, 1920.